

# THE $t$ - $J_z$ LADDER

A. Weiße, R. J. Bursill, C. J. Hamer and Zheng Weihong<sup>1</sup>

<sup>1</sup>*School of Physics, The University of New South Wales, Sydney, NSW 2052, Australia*

(Dated: January 30, 2019)

The phase diagram of the two-leg  $t$ - $J_z$  ladder is explored, using the density matrix renormalization group method. Results are obtained for energy gaps, electron density profiles and correlation functions for the half-filled and quarter-filled cases. The effective Lagrangian velocity parameter  $v_\rho$  is shown to vanish at half-filling. The behaviour of the one-hole gap in the Nagaoka limit is investigated, and found to disagree with theoretical predictions. A tentative phase diagram is presented, which is quite similar to the full  $t$ - $J$  ladder, but scaled up by a factor of about two in coupling. Near half-filling a Luther-Emery phase is found, which may be expected to show superconducting correlations, while near quarter-filling the system appears to be in a Tomonaga-Luttinger phase.

PACS numbers: 03.70+k,11.15.Ha,12.38.Gc

(Submitted to Phys. Rev. D)

## I. INTRODUCTION

The discovery of high-temperature superconductivity in the cuprate materials has sparked huge interest in models of strongly correlated electrons in low-dimensional systems, such as the Hubbard,  $t$ - $J$  and  $t$ - $J_z$  models. These models are exactly solvable in one dimension, at least in some special cases; but the two-dimensional models pose a formidable numerical challenge. The ‘minus sign’ problem is a major stumbling block for Monte Carlo calculations in these fermionic systems; and the convergence of Density Matrix Renormalization Group (DMRG) calculations is slow in two dimensions. Exact finite-lattice calculations are limited to small lattice sizes; while series expansions have typically only been useful for special cases such as the half-filled limit.

In these circumstances, a considerable effort has been invested in the study of ‘ladder’ systems consisting of two or more coupled chains of sites. Ladders provide a ‘half-way house’, in some sense, between one and two dimensions; and they also display some very interesting effects in their own right [1, 2]. They display quite different behaviour depending on whether the number of legs is even or odd, as in the Haldane effect for the Heisenberg ladders [3]. Furthermore, experimental compounds have been found which form ladders [4], such as  $\text{SrCu}_2\text{O}_3$  [5], which may allow the theoretical predictions to be tested experimentally.

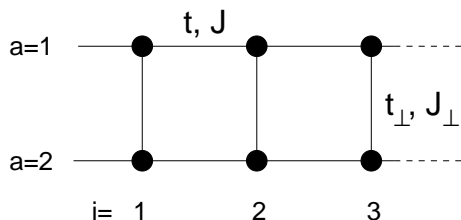
The  $t$ - $J$  model is an ‘effective Hamiltonian’ for the parent Hubbard model, valid when the Coulomb repulsion is large, but nowadays it is considered as an interesting model in its own right [6, 7]. The  $t$ - $J_z$  model is a variant in which the rotational symmetry is broken, and the spin interactions are Ising-like. The two-leg  $t$ - $J$  ladder has been extensively studied, using exact diagonalization [8, 9, 10, 11, 12, 13, 14, 15], quantum Monte Carlo [16], the DMRG technique [17, 18, 19, 20, 21, 22, 23], a combination of different methods [24], or using mean-field

or approximate analytic methods [18, 25, 26, 27]. Near half-filling, the model has been explored using dimer series expansions [28, 29, 30].

Our object is to study the corresponding two-leg  $t$ - $J_z$  ladder, and compare the results for the two models. This model has not been studied before, as far as we are aware, but the  $t$ - $J_z$  chain has been discussed by Batista and Ortiz [31], and the  $t$ - $J_z$  model on the square lattice has been treated by several groups [32, 33, 34, 35]. Our primary tool is the DMRG approach, supplemented with a few series calculations near half-filling.

The phase diagram for the  $t$ - $J$  ladder has been discussed by Troyer et al. [10], Hayward and Poilblanc [12], and Müller and Rice [14]. At large  $J/t$ , the holes all clump together, and phase separation occurs into hole-rich and hole-poor regions. At intermediate  $J/t$ , near half-filling, a ‘C1S0’ or Luther-Emery phase occurs, where the spin excitations are gapped, while there is a gapless charge excitation mode. Troyer et al. [10] found evidence of pairing between the holes in this region, together with long-range superconducting correlations with modified d-wave symmetry. The spin gap is discontinuous at half-filling, as the simple magnon excitation gives way to a particle-hole excitation with spin. At smaller  $J/t$ , the phase structure appears to become more complicated, with a possible C2S2 phase appearing (two gapless charge modes and two gapless spin modes) [14]; while at extremely small  $J/t$ , a Nagaoka phase is expected to appear [36], where each hole is surrounded by a region of ferromagnetic spins, forming a ferromagnetic polaron. In that region no spin gap occurs, and the holes repel each other.

The  $t$ - $J_z$  ladder might be expected to show similar behaviour. The major difference between the models is that quantum spin fluctuations are absent in the  $t$ - $J_z$  model, and the system exhibits long-range antiferromagnetic order for half-filling at  $T = 0$ , whereas the  $t$ - $J$  model does not. This long-range order will be destroyed at any finite temperature, however, and both models will then display similar long-range antiferromagnetic correlations. The

FIG. 1: The  $t$ - $J$  ladder.

two models should be very similar in most other aspects.

This expectation is borne out by our numerical results. The phase diagram for the  $t$ - $J_z$  ladder looks very similar to that of the  $t$ - $J$  ladder, except that the critical couplings are about twice as large, and the Tomonaga-Luttinger C1S1 phase extends to somewhat higher electron densities.

In Section II we specify the model, and consider its behaviour in various limiting cases. In Section III a brief discussion of the DMRG method is given, and in Section IV our numerical results are presented. Our conclusions are given in Section V.

## II. THE MODEL

The Hamiltonian of the  $t$ - $J_z$  ladder model is (see Figure 1)

$$\begin{aligned}
 H = & J \sum_{i,a} S_{ia}^z S_{i+1,a}^z + J_{\perp} \sum_i S_{i1}^z S_{i2}^z \\
 & -t \sum_{i,a,\sigma} P(c_{ia\sigma}^{\dagger} c_{i+1,a\sigma} + h.c.) P \\
 & -t_{\perp} \sum_{i,\sigma} P(c_{i1\sigma}^{\dagger} c_{i2\sigma} + h.c.) P
 \end{aligned} \quad (1)$$

Here the index  $a = 1, 2$  labels the two legs of the ladder,  $i$  labels the rungs of the ladder, the couplings  $J, J_{\perp}$  are the strengths of the spin interactions on legs and rungs respectively, and  $t, t_{\perp}$  are the hopping strengths on legs and rungs. The projection operators  $P$  forbid double occupancy of sites as usual. A density-density interaction term is sometimes included as a relic of the parent Hubbard model, but we do not do that here.

In the half-filled case, with a single electron occupying every site ( $n=1$ ), the model becomes equivalent to a simple classical Ising antiferromagnet. The ground state is a doubly degenerate antiferromagnetic state (Fig. 2a), with energy

$$E_0 = -\frac{L}{4}(2J + J_{\perp}), \quad (2)$$

where  $L$  is the number of rungs of the ladder.

The system can be solved exactly in various limiting cases:

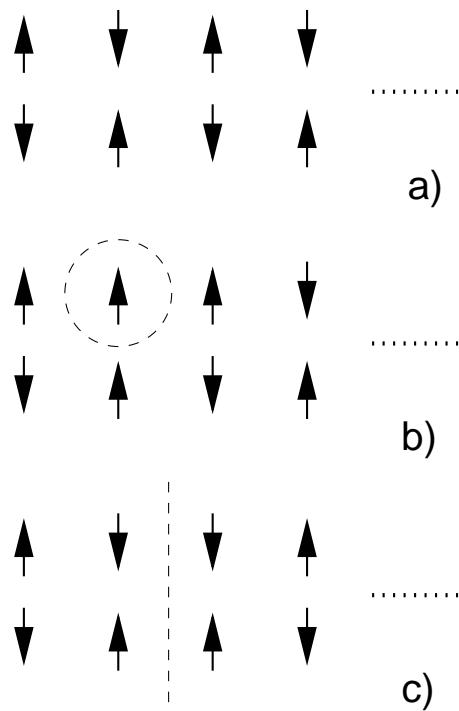


FIG. 2: Spin configurations at 1/2 filling: a) the antiferromagnetic ground state; b) an  $S^Z = 1$  excitation; c) a domain wall ('soliton') excitation.

TABLE I: Rung dimer eigenstates.

Number	Eigenstate	$S^z$	Energy	
1	$( \uparrow\downarrow\rangle -  \downarrow\uparrow\rangle)/\sqrt{2}$	0	$-J_{\perp}/4$	'singlet'
2	$ \uparrow\uparrow\rangle$	1	$+J_{\perp}/4$	
3	$( \uparrow\downarrow\rangle +  \downarrow\uparrow\rangle)/\sqrt{2}$	0	$-J_{\perp}/4$	'triplet'
4	$ \downarrow\downarrow\rangle$	-1	$+J_{\perp}/4$	
5	$ 00\rangle$	0	0	hole-pair singlet
6	$( \uparrow 0\rangle +  0 \uparrow\rangle)/\sqrt{2}$	1/2	$-t_{\perp}$	electron-hole
7	$( 0 \downarrow\rangle +  \downarrow 0\rangle)/\sqrt{2}$	-1/2	$-t_{\perp}$	bonding
8	$( \uparrow 0\rangle -  0 \uparrow\rangle)/\sqrt{2}$	1/2	$+t_{\perp}$	electron-hole
9	$( 0 \downarrow\rangle -  \downarrow 0\rangle)/\sqrt{2}$	-1/2	$+t_{\perp}$	antibonding

### 1. The rung dimer limit ( $J/J_{\perp} \rightarrow 0, t/J = t_{\perp}/J_{\perp}$ )

For  $J_{\perp} \gg J$ , the system consists of independent dimers on the rungs of the ladder. The eigenstates on a single rung are listed in Table I. The ground state is doubly degenerate here, with both 'singlet' and 'triplet' states with  $S^z = 0$  having the same energy, unlike the case of the full  $t$ - $J$  ladder. This degeneracy means that one cannot simply compute a perturbation series expansion about the dimer limit in this case, unless one employs degenerate perturbation theory, or introduces an 'artificial' interaction to lift the degeneracy.

### 2. The independent chain limit ( $J_{\perp}/J \rightarrow 0, t/J = t_{\perp}/J_{\perp}$ )

In this case we end up with two independent chains. The chain behaviour has been discussed by Batista and Ortiz [31]. They showed that the spins were Néel ordered along the chain in the ground state, which could then be mapped onto an XXZ spin chain. Phase separation occurs at the (rather large) value  $J/t = 8$  for all hole densities. Below that value, the system forms a gapless Luttinger liquid, with correlation exponent  $K_{\rho}$  and charge velocity  $v_{\rho}$ . The system can be exactly solved via the Bethe ansatz, at quarter filling giving

$$K_{\rho} = \frac{\pi}{4(\pi - \mu)}, \quad v_{\rho} = \frac{\pi t \sin \mu}{\mu} \quad (3)$$

where  $\cos \mu = -J/8t$ . Thus for  $0 \leq J/8t \leq 1/\sqrt{2}$ , we have  $1/\sqrt{2} \leq K_{\rho} \leq 1$ , while for  $1/\sqrt{2} \leq J/8t \leq 1$ , we have  $K_{\rho} > 1$ , implying that superconducting correlations dominate at large distances. At half filling, on the other hand, we have free fermion (metallic) behaviour with  $K_{\rho} = 1/2$ .

### 3. The Ising limit ( $t/J \rightarrow 0, t/J = t_{\perp}/J_{\perp}$ )

In this limit, the model becomes equivalent to a classical, static Ising model. Unless otherwise stated, we assume periodic boundary conditions, and an even number of rungs  $L$ . The ground state at half-filling is the fully antiferromagnetic state shown in Figure 2a, with  $S^z = 0$ . The low-energy spin excitations will consist either of localized flipped spins ('magnons') with  $S^z = \pm 1$ , as shown in Fig. 2b, or else domain wall ('soliton') excitations, as shown in Fig. 2c, analogous to the 'spinon' excitations in Heisenberg chains, but carrying  $S^z = 0$  in this case. The total number of solitons, in the absence of holes, and assuming periodic boundary conditions, has to be even for  $L$  even, and odd for  $L$  odd, as in the Heisenberg chain. The energy gaps for these two excitations are respectively

$$\begin{aligned} E_{2b) - E_0} &= J + \frac{J_{\perp}}{2} \\ E_{2c) - E_0} &= J \end{aligned} \quad (4)$$

Since there are no quantum spin fluctuation terms in the Hamiltonian, these spin excitations are of course static, in the absence of holes. Note that since the solitons carry integer spin, there is no possibility of spin-charge separation in this model.

The lowest-energy charge excitation will consist of a single hole in the antiferromagnetic background (Fig. 3a), with spin  $S^z = \pm 1/2$ , and energy

$$E_{3a) - E_0} = \frac{1}{4}(2J + J_{\perp}) \quad (5)$$

The lowest eigenstates in the 2-hole sector consist of a bound pair on adjacent sites (Figs. 3b,3c), with spin

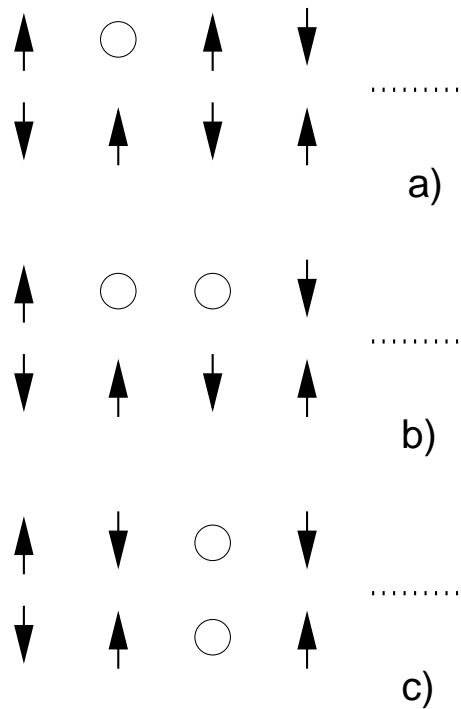


FIG. 3: Charge excitations near to 1/2 filling: a) a 1-hole state; b),c) 2-hole states.

$S^z = 0$  and energies

$$\begin{aligned} E_{3b) - E_0} &= \frac{1}{4}(3J + 2J_{\perp}) \\ E_{3c) - E_0} &= \frac{1}{4}(4J + J_{\perp}) \end{aligned} \quad (6)$$

It is clear that holes will cluster together to minimize the number of 'broken bonds' and hence the energy, and the system will be phase separated in this Ising limit.

For small but finite  $t/J$ , one can study the system via perturbation series calculations in  $t/J$ . Some results of these calculations will be shown in later sections. The single hole states illustrated in Fig. 3a are localized states, because there is an energy barrier preventing them from hopping: any hop will disturb the antiferromagnetic alignment of the spins. At higher energy, however, there will be states such as that shown in Figure 4, with unperturbed energy

$$E_4 - E_0 = \frac{1}{4}(8J + J_{\perp}), \quad (7)$$

where the hole is free to hop along the zig-zag path shown without incurring any further penalty in spin interaction energy. Assuming periodic boundary conditions, these states are made up of a hole plus a soliton for  $L$  even, or a hole alone for  $L$  odd. For finite  $t/J$ , they will form a band of itinerant electron states. The mobility of the electrons in both the chain and the ladder systems is a major point of distinction from the two-dimensional model, where the holes are 'confined', i.e. cannot move without creating a

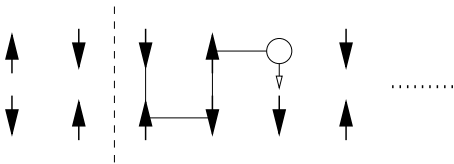


FIG. 4: A hole-plus-domain-wall excitation, showing an allowed zig-zag path for hopping (solid line).

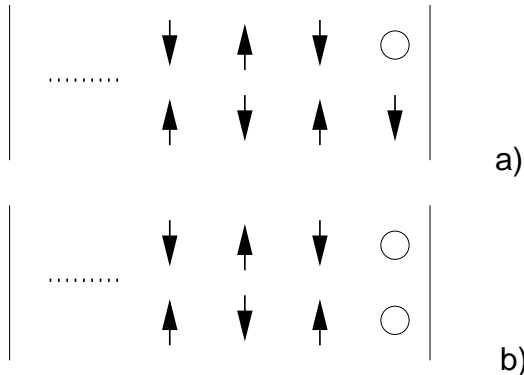


FIG. 5: Charge excitations for the ladder with open boundaries: a) 1 hole; b) 2 holes.

‘string’ of overturned spins behind them, and paying a penalty in spin interaction energy [37]. The states (3a) and (4) will mix as soon as  $t$  is turned on, and both configurations should be regarded as hole-soliton bound states.

We will also employ open boundary conditions in our calculations. In this case, the holes will cluster towards the boundaries in the Ising limit, in order to minimize the number of broken bonds. In this case the ground-state energy is

$$E_0 = -\frac{1}{4}(2J(L-1) - LJ_{\perp}), \quad (8)$$

and the lowest 1-hole state (Fig. 5a) has energy

$$E_{5a) - E_0 = \frac{1}{4}(J + J_{\perp}), \quad (9)$$

while the lowest 2-hole state (Fig. 5b) has energy

$$E_{5b) - E_0 = \frac{1}{4}(2J + J_{\perp}). \quad (10)$$

The single hole state is not necessarily accompanied by a soliton in this case.

#### 4. The free-fermion limit ( $J/t \rightarrow 0, t/J = t_{\perp}/J_{\perp}$ )

In this limit, a single hole will move through the lattice as a free particle, and its dispersion relation is naively expected to be

$$E_1(k) = -2t \cos k - t_{\perp} \quad (11)$$

For simplicity, we shall restrict our remarks henceforth to the isotropic case  $t_{\perp} = t$ , when the 1-hole energy gap in this limit is  $-3t$ .

The behaviour at small  $J/t$  should be similar to that of the  $t$ - $J$  model. The 1-hole energy in the two-dimensional  $t$ - $J$  model has been discussed by a number of authors [32, 37, 38, 39, 40]. At extremely small  $J/t$  (of order  $10^{-2}$ , in the region of the Nagaoka phase [36, 40]), the hole will be surrounded by a ferromagnetic ‘polaron’, or region of ferromagnetically aligned spins, with spin energy of order  $JR^2$  for a disc of radius  $R$ , within which the hole is fully mobile. In this regime, the 1-hole energy is

$$E_{1h}/t \sim -4 + c_1 \left(\frac{J}{t}\right)^{1/2} \quad (12)$$

where  $c_1$  is a numerical constant. At larger  $J/t$ , however, the lowest-energy states correspond to Brinkman-Rice ‘string’ states [37, 38], where the hole is confined by a ‘string’ of overturned spins within an antiferromagnetic background. This picture gives a 1-hole energy

$$E_{1h}/t \sim -a_1 + b_1 \left(\frac{J}{t}\right)^{2/3} \quad (13)$$

where  $a_1 < 4$ . Shraiman and Siggia [38] estimated  $a_1 = 2\sqrt{3}$  and  $b_1 = 2.74$  for the  $t$ - $J_z$  model, quite close to the values found numerically by Barnes et al [32], and White and Affleck [40].

For a one-dimensional chain, no Nagaoka phase occurs, but for a ladder the condition is once again met that holes can hop around closed loops, and a Nagaoka phase is expected [10]. White and Affleck [40] have pointed out that the ferromagnetically aligned spins inside the polaron will orient themselves in the  $xy$  plane, rather than along the  $z$  axis, because this costs an exchange energy of  $J/4$  per bond, rather than  $J/2$ . For our ladder model, the ferromagnetic ‘polaron’ region will be one-dimensional. If the polaron region spans  $L$  rungs of the ladder, the cost in magnetic energy will be

$$E_M = \frac{3}{4}JL \quad (14)$$

Assuming the 1-hole wavefunction to vanish at the edges of the polaron, it will take the form

$$|\psi_k\rangle = A \sum_n \cos(kn)(|n, 1\rangle + |n, 2\rangle), \quad k = \frac{\pi}{L} \quad (15)$$

where  $|n, a\rangle$  denotes a hole at rung  $n$  on leg  $a$  of the ladder, and  $A$  is a normalization constant. The kinetic or hopping energy is then easily found to be

$$E_K = -3t + t\left(\frac{\pi}{L}\right)^2 \quad (L \rightarrow \infty) \quad (16)$$

Minimizing the total energy  $E_{1h} = E_M + E_K$  with respect to  $L$  we find

$$\begin{aligned} E_{1h}/t &= -3 + \frac{3}{4}\left(\frac{3\pi J}{t}\right)^{2/3} \\ &= -3 + 3.35(J/t)^{2/3} \end{aligned} \quad (17)$$

For intermediate  $J/t$ , the Brinkman-Rice string picture [37, 38] will give a qualitatively similar behaviour

$$E_{1h}/t \sim -a_2 + b_2 \left(\frac{J}{t}\right)^{2/3} \quad (18)$$

where  $a_2 < 3$ . It is doubtful whether approximations such as those used by Shraiman and Siggia [38] to calculate the coefficients  $a_2$  and  $b_2$  for the 2D model are at all accurate for the ladder, and we will not attempt an explicit calculation of these coefficients.

### A. The Effective Hamiltonian

In the regime of physical interest, the  $t$ - $J$  ladder is believed to be in a C1S0 or Luther-Emery phase, with gapped spin excitations and gapless charge excitations corresponding to bound hole pairs. Several authors [10, 12, 21, 22] have discussed an effective Hamiltonian to describe these bosonic excitations, which would capture the low-energy physics of the model. Here we merely summarize their results.

In the recent analysis of White, Affleck and Scalapino [22], they use a bosonization technique to construct the low-energy effective Hamiltonian

$$H - \mu L = \frac{v_\rho}{2} \int dx [K_\rho \Pi_\rho^2 + \frac{1}{K_\rho} (\frac{d\theta_\rho}{dx})^2] \quad (19)$$

where  $\mu$  is a chemical potential,  $\Pi_\rho$  is the momentum density conjugate to  $\theta_\rho$ ,  $v_\rho$  is the velocity of the corresponding gapless low-energy excitations and the parameter  $K_\rho$  controls the correlation exponents. The two parameters  $v_\rho$  and  $K_\rho$  must be extracted from numerical data.

White et al. [22] show that the finite-size scaling behaviour of a general low-energy excitation is

$$E - E_0 = -2p\mu + \frac{2\pi v_\rho}{L} [K_\rho m^2 + \frac{p^2}{4K_\rho} + \sum_{k=1}^{\infty} k(n_{Lk} + n_{Rk})] \quad (20)$$

where  $E_0$  is the ground-state energy for a given density  $n$ ,  $n_{Lk}$  and  $n_{Rk}$  are occupation numbers for left and right moving states of momentum  $2\pi k/L$ ,  $L$  is the number of rungs of the ladder, and  $p$  and  $m$  are integer-valued quantum numbers. The total charge relative to the ground state is  $Q = -2p$ , and the other quantum number  $m$  measures the ‘‘chiral charge’’.

By measuring the ground-state energies for three different charge states with  $\Delta Q = \pm 2$ , one can determine the ratio  $v_\rho/K_\rho$ :

$$E(p=1) + E(p=-1) - 2E_0 = \frac{\pi v_\rho}{K_\rho L} \quad (21)$$

This is directly related to the electron compressibility  $\kappa$  of the two-leg ladder, generally defined as

$$\frac{1}{n^2 \kappa} \equiv \frac{1}{2L} \frac{d^2 E}{dn^2} = \frac{\pi v_\rho}{2K_\rho} \quad (22)$$

using (21), where  $n$  is the electron density. This formula applies for either periodic or open boundary conditions, in principle. The velocity may be measured independently using the excitation energy of the lowest state of momentum  $2\pi/L$  for periodic BC

$$E(n_{R1}=1) - E_0 = \frac{2\pi v_\rho}{L} \quad (23)$$

For open BC, the momentum spacing is  $\pi/L$ , and the corresponding formula is

$$E(n_1=1) - E_0 = \frac{\pi v_\rho}{L} \quad (24)$$

Hence one can obtain estimates for  $K_\rho$  and  $v_\rho$  separately.

One may also use ‘twisted’ boundary conditions with the wave function acquiring a phase  $\Phi$  at the boundary, corresponding to an Aharonov-Bohm flux threading the one-dimensional ring formed by joining the ends of the ladder together. This increases the ground-state energy by

$$E_0 \rightarrow E_0 + \frac{8\pi v_\rho K_\rho \Phi^2}{L} \quad (25)$$

and allows one to determine the combination  $v_\rho K_\rho$ . This approach was used by Hayward and Poilblanc [12].

Finally, White et al. [22] discuss how one may estimate  $K_\rho$  from the decay of Friedel oscillations in the system. Friedel oscillations are density oscillations produced near the boundary of an open ladder, which decay with a power law corresponding to the exponent  $K_\rho$  with distance into the ladder. Using their bosonization analysis and a conformal transformation, White et al [22] show that for a system of length  $L$  the density at site (rung)  $j$  should vary as

$$\langle n_j \rangle \rightarrow \frac{C \cos(2\pi n j + \beta)}{[(2L/\pi) \sin(\pi j/L)]^{K_\rho}} \quad (26)$$

where  $C, \beta$  are constants, and  $2\pi n$  is the minimum wave vector of Friedel oscillations in the C1S0 phase, corresponding to two holes per wavelength. This is the same wave vector that would occur for a one-component spinless hard core bose gas, made up of tightly bound hole pairs.

Schulz [41] has argued in the case of the  $t$ - $J$  ladder that  $K_\rho$  should take the universal value  $K_\rho = 1$  at half-filling; but his argument starting from the rung dimer limit is not necessarily applicable to the  $t$ - $J_z$  model.

Note that the picture may be complicated by the occurrence of a gapped charge density wave (CDW) phase at special commensurate filling factors such as  $n = 0.5$  or  $n = 0.75$ . In this case, the charge density oscillations persist at all distances from the walls, corresponding to broken translational symmetry and a regular pattern of hole placements. This possibility has been discussed by Riera et al [35] and White et al [22].

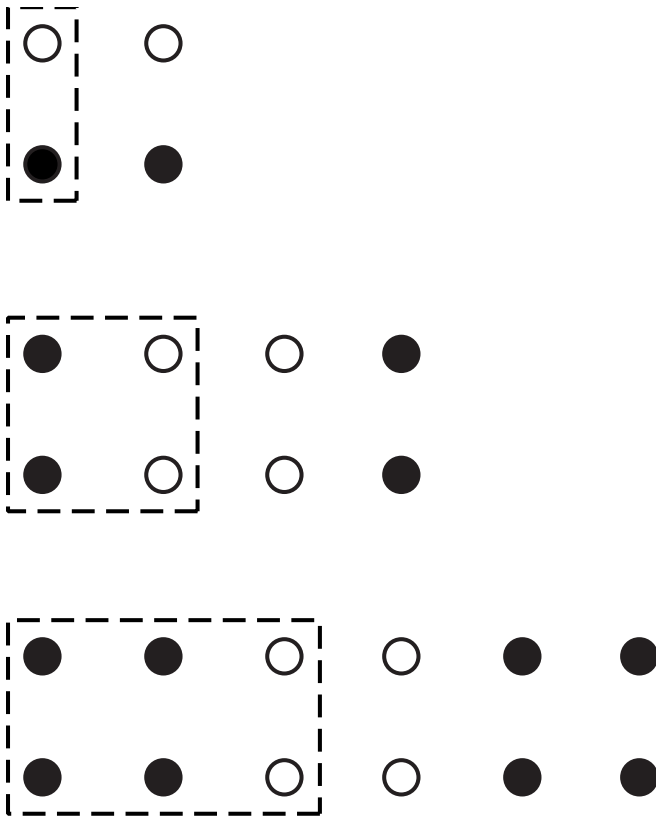


FIG. 6: Infinite lattice construction of the two-leg ladder. Two whole rungs (four sites—open circles) are added per DMRG step. The system and environment blocks increase by one rung (two sites) per DMRG step.

### III. METHOD

The model (1) is solved using the Density Matrix Renormalisation Group (DMRG) method [42]. Calculations have been performed at both half-filling and quarter-filling. Calculations have been performed with both periodic and open boundary conditions in the horizontal direction, but most of the results use OBCs because the convergence is much better in this case.

In the half-filled case we have calculated the ground state as well as one, two and four-hole excited states. In the one-hole case we have calculated  $S^z = 1/2, 3/2$  and  $5/2$  states. We have calculated energies of these states as well as density profiles  $\langle \hat{n}_i \rangle$ . The infinite lattice algorithm [42] is employed in this case, using typically  $M = 60$  states per block and symmetry sector, which corresponds to a total of about 300 system block states. The lattice build-up phase is illustrated in Fig. 6. By running tests for a number of different values of  $M$ , we established that the energies of these states have been resolved with sufficiently high accuracy for our purposes.

In the quarter-filled case, it is necessary to use the finite lattice method [42] in order to achieve reasonably converged energies. We use the infinite lattice method to build a ladder to a given size, increasing the system

block size by a whole rung at each DMRG step as in Fig. 6. We then perform a finite lattice sweep at the fixed lattice size, using the previously developed system blocks to improve the accuracy of the calculation. Once a target size has been completed with a finite lattice sweep, the infinite lattice algorithm is resumed to proceed to a larger target lattice size whereupon the sweeping procedure is again employed. This way we obtain accurate finite lattice method results for a number of lattice sizes, e.g.,  $N = 4, 8, 12, 16, 24, 32, 64, 128, 256$  lattice sites. Whenever necessary, the data are extrapolated to the bulk limit  $N \rightarrow \infty$  by fitting a low-order polynomial in  $1/N$  to the finite-lattice data.

## IV. RESULTS

We have calculated numerical DMRG results for this model for the isotropic case,  $J = J_\perp \equiv J_z, t = t_\perp$ , and for various  $J_z/t$ , on lattices of  $L$  rungs with  $L$  even. Our discussion henceforth will be limited to this case.

### A. Near Half-Filling

We begin by considering states with a finite number of holes doped into the half-filled system ( $n=1$ ).

#### 1. Single-hole states

Figure 7 shows DMRG estimates of the energy gap for a single hole with spin  $S^z = 1/2$ , as a function of  $J_z/t$ , for both periodic and open boundary conditions. The results of a series calculation are also shown for the periodic case. The series estimates were obtained assuming the Nagaoka form (17)

$$f(t) \equiv E_{1h} + 3t \sim bt^{1/3} \quad \text{as } t \rightarrow 0. \quad (27)$$

Accordingly, the series in  $t$  for  $f(t)$  was Euler transformed  $z = t/(1+t)$  to bring the singularity to  $z = 1$ ; then a further change of variable was made

$$1 - \delta = (1 - z)^{1/3} \quad (28)$$

so that one may treat the function  $(1 - \delta)f(\delta)$  as analytic in  $\delta$  near  $\delta = 1$ ; and finally, differential approximants were used to extrapolate this function to  $\delta = 1$ . It can be seen that the series results agree very well with the DMRG results for  $J - z/t > 0.3$ , but run a little lower below that.

It can also be seen that there is a difference between the DMRG results with periodic and open boundary conditions. As discussed in Section II 3, this is because the state with periodic boundary conditions is actually a hole-soliton bound state. The difference between the two energies is shown in the inset to Figure 7.

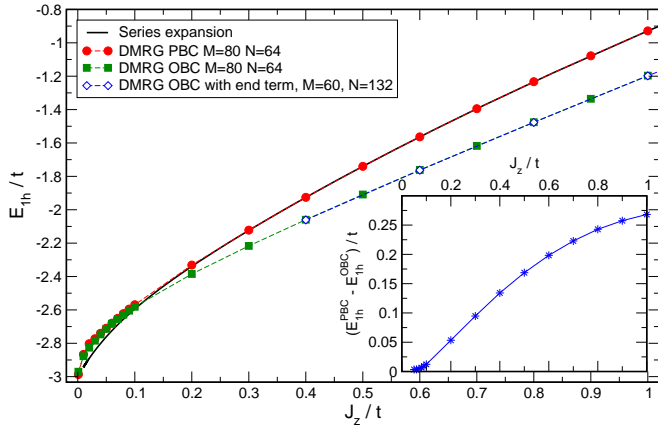


FIG. 7: (Colour online) The energy gap  $E_{1h}/t = (E_1 - E_0)/t$  for one hole, as a function of  $J_z/t$ . Filled circles, open boundary conditions; open squares, periodic boundary conditions; dashed line, estimates from Ising series expansion.

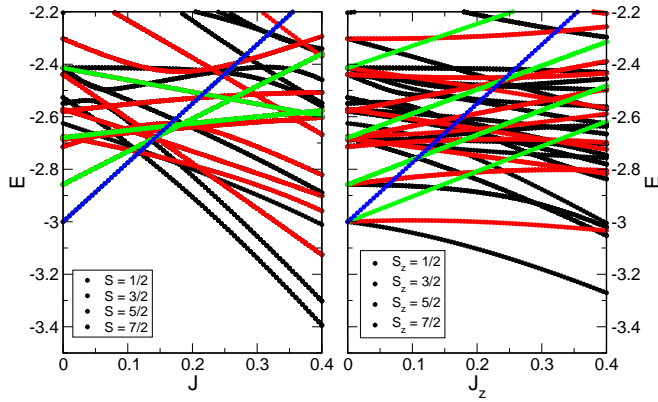


FIG. 8: (Colour online) Low energy spectrum of the  $t$ - $J$  (left) and  $t$ - $J_z$  (right) model on a 4-rung ladder with 7 electrons.

At smaller  $J_z/t$ , one is tempted to look for a transition to a Nagaoka phase [36], i.e. a phase with ferromagnetic spin order or at least a ferromagnetic polaron bubble around the hole. In the  $t$ - $J_z$  model, however, the situation is rather different from the  $t$ - $J$  model, where the full spin-rotation symmetry applies. The scenario is illustrated in Figure 8, where we show the complete 1-hole energy spectrum of the  $t$ - $J$  and  $t$ - $J_z$  models on a 4-rung cluster. The left-hand panel shows the  $t$ - $J$  case, where at  $J = 0$  the ground state has maximal spin  $S = 7/2$  (ferromagnetic). As  $J$  increases, at some critical coupling  $J_c$  this state crosses another state with minimal spin  $S = 1/2$ , which becomes the ground state thereafter. The right-hand panel shows the  $t$ - $J_z$  case. At  $J_z = 0$ , the system is rotation symmetric, the Nagaoka theorem applies and the ground state again has the maximal possible spin  $S_{\max}$  and degeneracy  $2S_{\max} + 1$ . As soon as  $J_z$  becomes finite, however, the symmetry is broken, the multiplet splits into its  $S^z$  components, and the state with minimal  $S^z = \pm 1/2$  becomes the ground state. Clearly, there is no level crossover in the  $t$ - $J_z$  case. All

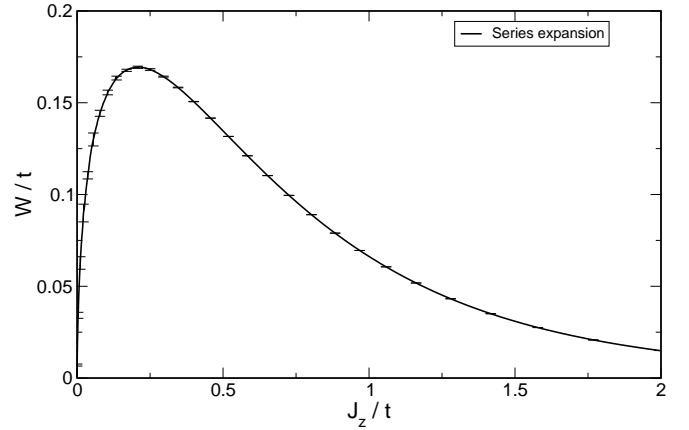


FIG. 9: The 1-hole bandwidth  $W/t$  as a function of  $J_z/t$ , estimated from the Ising series expansion.

we can expect for increasing  $J_z$  is a continuous fading-out of the ferromagnetic correlations. This accords with the smooth approach of the 1-hole energy to  $-3$  as  $J_z \rightarrow 0$  in Figure 7.

A comparison of the numerical data at small  $J_z/t$  with the theoretical prediction (17) gives the following results. A Dlog Padé analysis of the series gives a rather inaccurate estimate of the exponent in the range 0.5 - 0.7, which would be consistent with  $2/3$ . A fit to the DMRG data over the range 0 - 0.1, however, gives

$$\frac{E_{1h}}{t} = -3 + 1.444 \left( \frac{J_z}{t} \right)^{0.53}, \quad (29)$$

with an exponent much closer to  $1/2$  than  $2/3$ . This is illustrated by the difference between the DMRG data and the series extrapolation in Figure 7 at small  $J_z/t$ . Thus the data do not seem to behave in accordance with theoretical expectations in this instance.

Figure 9 shows the bandwidth for the 1-hole state with  $S^z = 1/2$  predicted by the Ising series expansion, as a function of  $J_z/t$ . We see that the predicted bandwidth rises as  $J_z/t$  decreases, as one might expect, until at  $J_z/t \simeq 0.3$  it reaches a peak, and begins to drop towards zero. Similar behaviour in the region of small  $J/t$  has been predicted for the 2D  $t$ - $J$  model by Martinez and Horsch [43] and Liu and Manousakis [44], and confirmed by series calculations [45]. The theoretical predictions assume long-range antiferromagnetic order, and construct an effective Hamiltonian in which the spin dynamics are treated in linear spin-wave theory, and the holes are treated as spinless fermions, following Schmitt-Rink, Varma and Ruckenstein [46]. The results are consistent with the string picture of Brinkman and Rice [37], and appear to show a sequence of narrow ‘string’ excitation peaks in the spectral function, corresponding to holes bound in a linear potential. The effects are even more marked in the  $t$ - $J_z$  model.

It would be very interesting to check the actual behaviour of the bandwidth by means of DMRG estimates,

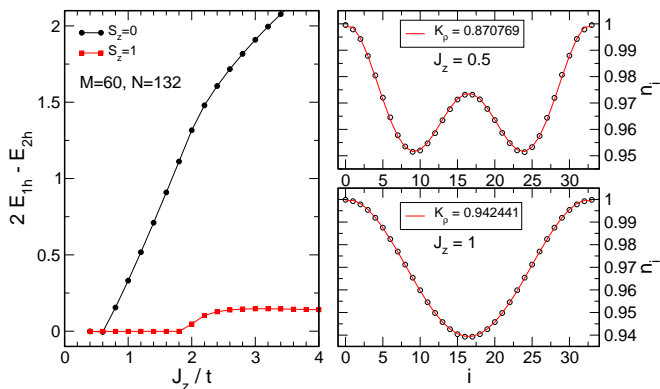


FIG. 10: (Colour online) Left: Two-hole binding energies as a function of  $J_z/t$ , calculated with OBC and finite boundary potentials. Filled circles:  $S^z = 0$ ; filled squares:  $S^z = 1$ . Right: Average electron number per rung as a function of distance along the ladder, for 2-hole states on a lattice of 34 rungs: a)  $J_z/t = 0.5$ ; b)  $J_z/t = 1.0$ . The lines are fits using equation (32).

but unfortunately our codes cannot distinguish different momentum eigenstates.

## 2. Two-hole states

In studying 2- and 4-hole states and looking for the phase separation boundary, we wanted to avoid the holes sticking to the boundary and thus obscuring the bulk physics. Accordingly, we have added an extra ‘boundary potential’ term at the sites adjacent to the boundary:

$$H_B = -\frac{J_z}{4} \sum_{i,\sigma} c_{i,\sigma}^\dagger c_{i,\sigma}. \quad (30)$$

As it turns out, this makes a negligible difference to the energy gaps in the region of interest.

In the 2-hole sector, the first quantity of interest is the 2-hole binding energy

$$E_B = 2E_1 - E_2 - E_0 \quad (31)$$

Figure 10 shows the binding energy as a function of  $J_z/t$  for both  $S^z = 0$  and  $S^z = 1$ , computed with open boundary conditions. It can be seen that a 2-hole bound state with  $S^z = 0$  forms for large  $J_z/t$ , but the binding energy vanishes at  $J_z/t \simeq 0.60$ , and below this point the holes do not bind. In the  $S^z = 1$  channel, there is a small binding energy at large  $J_z/t$ , which vanishes at  $J_z/t \simeq 1.8$ .

Similar results have been found for other members of this family of models. For the 2D  $t$ - $J_z$  model, Riera and Dagotto [33] estimated that the holes become unbound at  $J_z/t \simeq 0.18$ ; while for the  $t$ - $J$  ladder, Jurecka and Brenig [30] suggest that hole binding vanishes at  $J/t \simeq 0.5$ . There is binding in the  $S = 1$  channel for the  $t$ - $J$

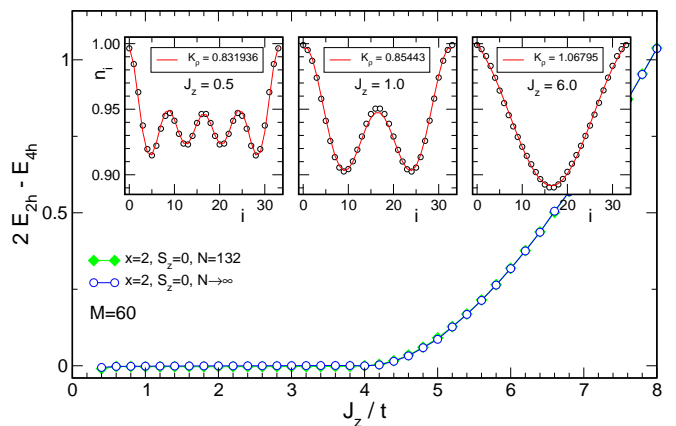


FIG. 11: (Colour online) Four-hole binding energy as a function of  $J_z/t$ , calculated with OBC and finite boundary potentials. Insets: Electron density profiles at characteristic values of  $J_z/t$ , together with fits to the corresponding Friedel expression.

ladder, but it is considerably smaller than in the  $S = 0$  channel.

Wherever the 2-hole binding energy is positive, we expect a continuous band of 2-hole bound states to appear above the ground state; so that within the 2-hole sector, particle-hole excitations (‘excitons’) can occur down to zero energy. In other words, excitons with  $S^z = 0$  are gapless, as found by Troyer et al [10] for the  $t$ - $J$  ladder.

We note that the spin energy gap between the  $S^z = 1$  and  $S^z = 0$  2-hole states also drops to zero at  $J_z/t = 0.6$ . It always remains below the  $S^z = 1$  ‘magnon’ energy  $3J/2$ ; or in other words, an exciton with  $S^z = 1$  in the 2-hole sector has an energy substantially below that of the magnon. Therefore the spin gap drops discontinuously as one moves away from half-filling, which again agrees with the behaviour found by Troyer et al. [10] for the  $t$ - $J$  ladder.

The right panels of Figure 10 show profiles of the electron density in the 2-hole state as a function of distance along the ladder, calculated for a lattice of 34 rungs with open boundary conditions. At low  $J_z/t$ , the two holes are unbound and separated from each other, forming two distinct troughs in the density profile (Fig. 10). At  $J_z/t \simeq 0.6$  a sharp crossover takes place, where the two holes bind together and form a single trough in the density profile. As it happens, both profiles can be fitted quite well with a Friedel oscillation form

$$\langle n_j \rangle = c_0 + \frac{c_1 \sin[2\pi(n + 1/2)j/(L + 1)]}{[(L + 1) \sin[\pi j/(L + 1)]]^{K_\rho}} \quad (32)$$

where  $n = 2$  and  $K_\rho = 0.87$  in case a) and  $n = 1$  and  $K_\rho = 0.92$  in case b).



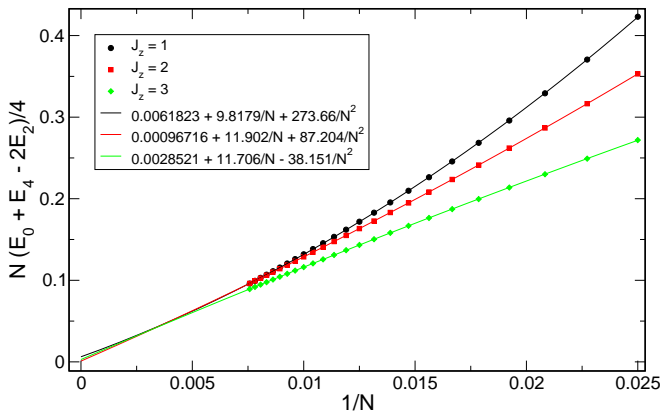


FIG. 12: (Colour online) Four-hole binding energy as a function of  $1/N = 1/(2L)$ , at  $J_z/t = 1, 2$  and  $3$ .

### 3. Four-hole states

The 4-hole binding energy for  $S^z = 0$  is shown as a function of  $J_z/t$  in Figure 11. It is finite at large  $J_z/t$ , and vanishes smoothly at  $J_z/t \simeq 4$ . This is taken to mark the point where phase separation occurs. The smooth behaviour of the binding energy may indicate a Kosterlitz-Thouless transition at this point. The insets show examples of the electron density profiles as functions of distance along the ladder for the 4-hole ground state. For  $J_z/t = 0.5$ , we see four separated holes; for  $J_z/t = 1.0$ , we see two separated hole-pairs; and for  $J_z/t = 6.0$ , we see a single 4-hole cluster, reinforcing the picture given above. Note that the Friedel form (32) again fits the density profiles remarkably well, upon choosing the appropriate value for  $n$ . The fits in the pair binding region indicate that the parameter  $K_\rho$  lies approximately in the range 0.8 - 1.0 near half-filling.

Next, we attempt to measure the isothermal compressibility in the non-phase-separated region, whose inverse is

$$\kappa^{-1} = n^2 N [E_4 + E_0 - 2E_2]/4 \quad (33)$$

where  $N = 2L$  is the number of sites, and  $n = (N-2)/N$  the electron density. Figure 12 shows  $\kappa^{-1}n^{-2}$  as a function of  $1/N$ , for some couplings  $J_z/t < 4$ , fitted by a quadratic polynomial in  $1/N$ . The extrapolations to the bulk limit  $N \rightarrow \infty$  are compatible with zero, indicating that the inverse compressibility vanishes at half-filling. This seems surprising at first sight, but the same result applies for the 1D  $t$ - $J$  chain at the integrable point [47]. Siller et al. [21] also found a tiny result for the inverse compressibility of the isotropic  $t$ - $J$  ladder near half-filling. The result can be understood as follows. The dispersion relation in the conduction band flattens out near the band edge, and hence the dispersion relation of a single hole at half filling is quadratic in momentum  $q$ , as illustrated by the free fermion equation 11 or the calculation of Sushkov [25] for the  $t$ - $J$  ladder. The dispersion relation for a bound hole-pair bosonic excitation

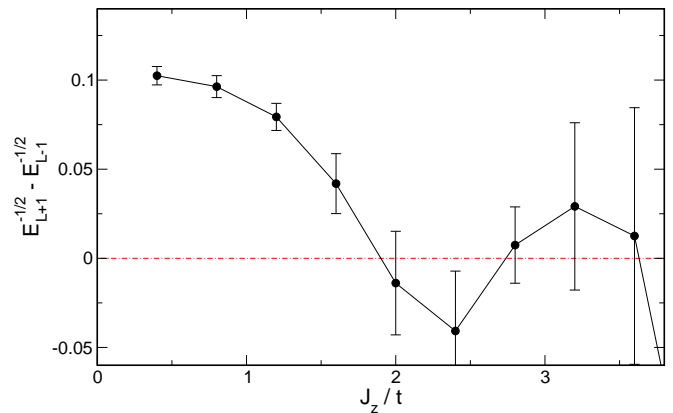


FIG. 13: The odd-even gap  $[E(n_h = L + 1, S^z = -1/2) + E(n_h = L - 1, S^z = -1/2) - 2E(n_h = L, S^z = 0)]/2$  at quarter-filling, as a function of  $J_z/t$ .

will likewise be quadratic in  $q$ . The vanishing of any term linear in  $q$  implies that  $v_\rho \rightarrow 0$  and Eq. (22) then leads to  $\kappa^{-1}n^{-2} = 0$ .

## B. Quarter Filling

Next we consider states at or near the quarter-filling point ( $n = 1/2$ ). Reliable results are very hard to obtain for  $J_z/t \geq 3$ . Phase separation presumably occurs in this region, so that the ground state becomes inhomogeneous, and very difficult to treat by DMRG methods. For the most part, our results will be for smaller  $J_z/t$ .

### 1. Odd-even gap

Figure 13 shows the energy gap between states with odd and even numbers of holes,  $[E(n_h = L + 1, S^z = -1/2) + E(n_h = L - 1, S^z = -1/2) - 2E(n_h = L, S^z = 0)]/2$ , where  $n_h$  is the number of holes, as a function of  $J_z/t$ . It can be seen that for  $J_z/t$  less than about 2.0, this gap is small and positive, but is consistent with zero beyond that point, within substantial errors. This behaviour is very similar to the two-hole gap shown in Figure 16. In fact it appears that the energy surface is quite smooth in this region, with little if any ‘corrugation’ between states with even or odd numbers of holes. This indicates that pairing effects between holes are weak or nonexistent in this region.

### 2. Spin Gap

Figure 14 shows the spin gap  $[E(n_h = L, S^z = 1) - E(n_h = L, S^z = 0)]$  as a function of  $J_z/t$ . The insert shows examples of the finite-size scaling behaviour of this quantity as a function of  $1/N$ , and the linear extrapolations made to the bulk limit. It can be seen that the

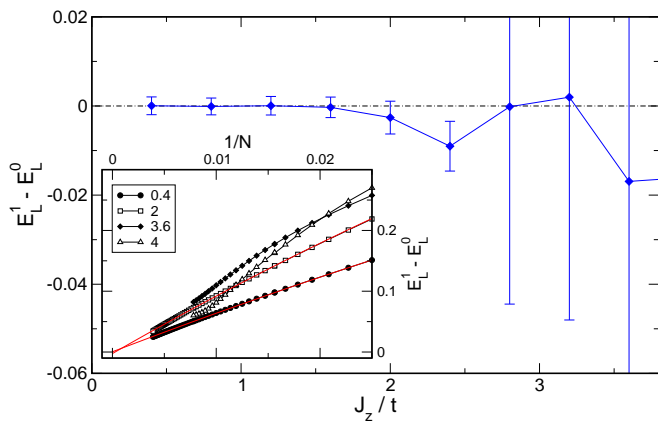


FIG. 14: The spin gap  $[E(n_h = L, S^z = 1) - E(n_h = L, S^z = 0)]$  at quarter-filling, as a function of  $J_z/t$ .

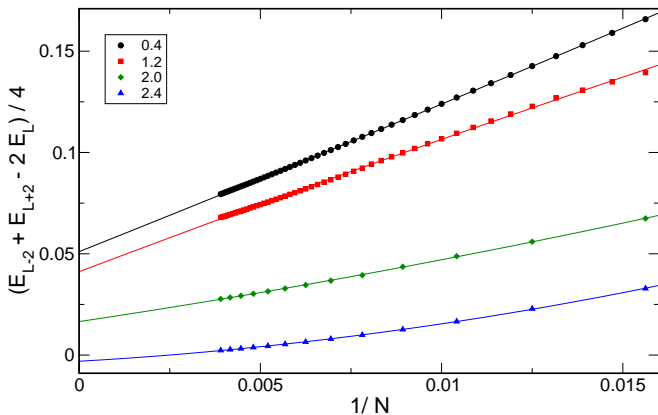


FIG. 15: The two-hole gap  $[E(n_h = L + 2, S^z = 0) + E(n_h = L - 2, S^z = 0) - 2E(n_h = L, S^z = 0)]/2$  at quarter-filling, as a function of  $1/N = 1/(2L)$ , at selected values of  $J_z/t$ .

results are consistent with zero over the whole region  $J_z/t \leq 4$ . Convergence for  $J_z/t > 2$  is not very good. Thus for  $J_z/t \geq 2.3$ , we appear to be in the C1S1 phase discussed by Hayward and Poilblanc [12] for the t-J ladder, where both the charge gap and the spin gap vanish.

### 3. Two-hole gap

Figure 15 shows the two-hole energy gap  $[E(n_h = L + 2, S^z = 0) + E(n_h = L - 2, S^z = 0) - 2E(n_h = L, S^z = 0)]$  as a function of  $1/N$  at selected values of  $J_z/t$ . For  $J_z/t \leq 2.3$ , the gap appears to scale to a finite value in the bulk limit  $N \rightarrow \infty$ , whereas the limit is consistent with zero from there on. Figure 16 shows the estimated bulk limit as a function of  $J_z/t$ . The finite charge gap for  $J_z/t < 2.3$  corresponds to a cusp in the energy density versus filling factor surface, and is evidence of the formation of a CDW state at this commensurate filling factor, according to White *et al.* [22].

We have looked for further evidence of the CDW state

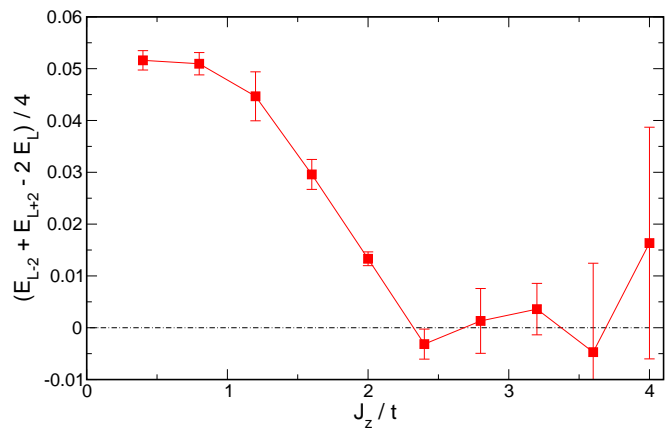


FIG. 16: The estimated two-hole gap in the bulk limit  $[E(n_h + L + 2, S^z = 0) + E(n_h = L - 2, S^z = 0) - 2E(n_h = L, S^z = 0)]/2$  at quarter-filling, as a function of  $J_z/t$ .

in the electron density profiles and correlation functions. The density profile on an odd-rung lattice at quarter filling shows some evidence of rung-to-rung oscillations, but they die away as  $N \rightarrow \infty$ , and so do not seem to correspond to the CDW.

Examples of the density-density correlation functions are shown in Figure 17, with one site fixed at the middle of the ladder, and the distance to the other site varying, including both sites on the same leg and those on the opposite leg of the ladder. There is a positive correlation for nearby sites, and a Friedel rung-to-rung oscillation near the boundary. In the intermediate region, there is no strong evidence of either a rung-to-rung alternation or a checkerboard alternation. One major qualitative difference is obvious, however, between Figures 17(a) and 17(c). At  $J_z/t = 2$ , the correlation function is virtually zero at intermediate and large distances, as one would expect of a solid phase: this is consistent with the CDW behaviour. For  $J_z/t = 3$ , on the other hand, the correlation function has a substantial dip at intermediate distances, which actually increases with increasing lattice size. This behaviour is more reminiscent of a liquid or a gas.

## V. DISCUSSION

As expected, the phase behaviour of the t- $J_z$  ladder at  $T = 0$  appears to be broadly similar to its counterpart, the t-J ladder. A schematic diagram is shown in Figure 18. At half-filling, the system is equivalent to an Ising antiferromagnet, with long range magnetic order; but at any finite temperature or hole density, the order parameter will vanish, leaving only finite-range antiferromagnetic correlations.

Near half-filling, phase separation into hole-rich and hole-poor regions occurs beyond  $J_z/t \simeq 4.0$ , which is about half the critical value for the t- $J_z$  chain [31], but twice the critical value for the full t-J ladder [10]. Below that, there is a C1S0 or Luther-Emery phase, where the

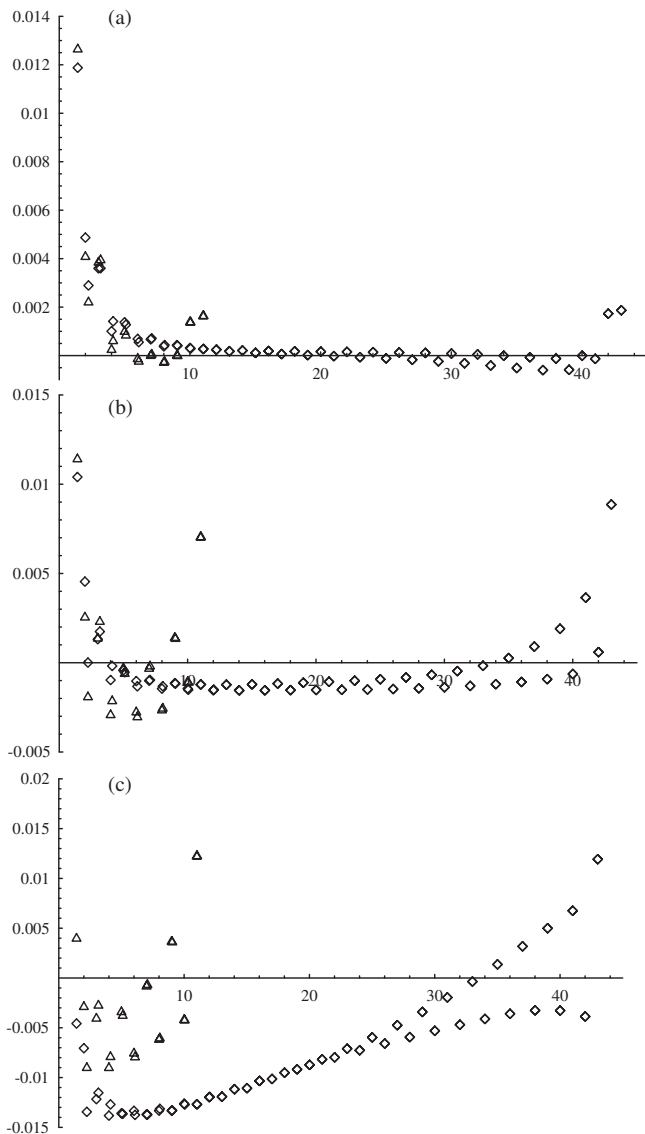


FIG. 17: The density-density correlation function as a function of distance, with one site fixed at the middle of the ladder and the other varying, at quarter filling. Triangles:  $L = 22$ ; squares:  $L = 88$ . Case a):  $J_z/t = 2.0$ ; b):  $J_z/t = 2.6$ ; c):  $J_z/t = 3.0$

holes bind into pairs and the charge gap vanishes, but the spin gap remains finite. The spin gap is discontinuous at half-filling, because the exciton spin gap is less than the magnon gap. These features are identical with those found for the  $t$ - $J$  model [10]. We have not explored the question whether there are superconducting correlations in this region, but they are expected to be present if  $K_\rho > 1/2$ .

The binding between hole pairs vanishes in the  $S^z = 1$  channel below  $J_z/t \simeq 1.8$ , and in the  $S^z = 0$  channel below  $J_z/t \simeq 0.6$ . Below that, the holes repel each other, and we presumably enter the C2S2 gapless phase discussed by Müller and Rice [14] for the  $t$ - $J$  case (although

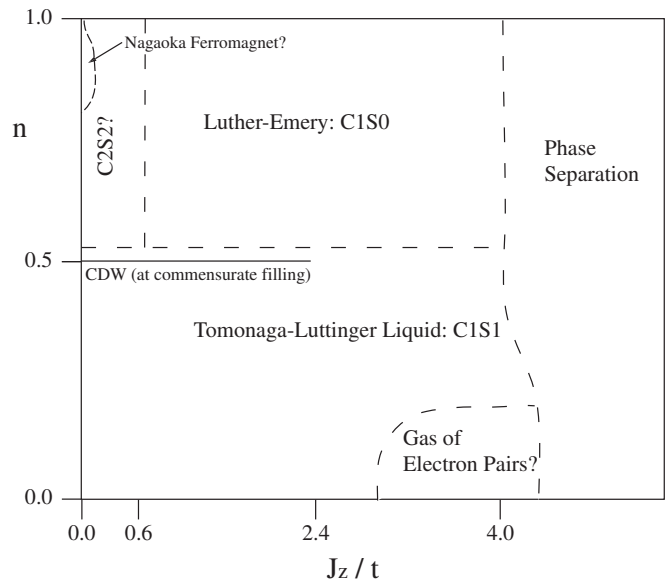


FIG. 18: Schematic phase diagram for the  $t$ - $J_z$  ladder.

exact diagonalization data up to  $N = 14$  are somewhat equivocal as to whether the  $S_z = 1$  states are degenerate). These different regimes are clearly evident in the hole density profiles on a finite lattice.

In the Nagaoka limit as  $J_z/t \rightarrow 0$ , a finite-lattice calculation reveals rather different behaviour in the two models in the one-hole sector. In the  $t$ - $J$  case, a state with maximal spin  $S$  crosses over the  $S = 1/2$  state to become the ground state as  $J/t \rightarrow 0$ . For the  $t$ - $J_z$  system, on the other hand, the  $S^z = 1/2$  state remains the ground state at all  $J_z/t$ , and the Nagaoka limit is approached smoothly. States with higher  $S^z$  become degenerate with the  $S^z = 1/2$  state in the limit, to form a multiplet with maximum total spin  $S$ . Any ferromagnetic correlations in the ground state appear to be transverse to the  $z$  direction, as argued by White and Affleck [40]. Our DMRG results for the one-hole gap appear to decrease as  $(J_z/t)^{1/2}$ , rather than  $(J_z/t)^{2/3}$  as predicted by theory; the theory needs re-examination for this case.

Some crude estimates of the effective Hamiltonian parameters in the Luther-Emery phase were made at half-filling. Friedel-type fits to the density profiles give  $K_\rho \simeq 0.8 - 1.0$ , although it is not clear that the Schulz argument [41] that  $K_\rho = 1$  at half-filling is applicable to the  $t$ - $J_z$  case. We found that  $v_\rho = 0$  in that limit, a general result which should apply to chains and ladders for both models.

We have also made some studies of the quarter-filled case. For  $J_z/t \leq 2.3$ , the system appears to be in a CDW state, with a finite two-hole gap and solid-like density-density correlation functions, although we could not discover any particular pattern of charge density waves. This behaviour was predicted for a commensurate filling factor by White, Affleck and Scalapino [22]. We find that the spin gap vanishes in this phase, and in fact is

compatible with zero at all couplings. For  $J_z/t \geq 2.3$ , any pairing effects are weak or nonexistent, and the system appears to be in a C1S1 Tomonaga-Luttinger phase with a single gapless spin and single gapless charge mode, similar to that discussed for the t-J ladder at densities at or below quarter-filling by Hayward and Poilblanc [12]. The calculations become very unstable beyond  $J_z/t \simeq 3$ , and we take this as indicating the onset of phase separation again at larger  $J_z/t$ . At very small electron densities, an electron-paired phase should exist. These findings are indicated schematically in Figure 18.

## Acknowledgments

This work forms part of a research project supported by a grant from the Australian Research Council. We are grateful for extensive computational support provided by the Australian Partnership for Advanced Computing (APAC) National Facility and by the Australian Centre for Advanced Computing and Communications (AC3).

- 
- [1] T.M. Rice, Z. für Physik B103, 165 (1997).  
 [2] E. Dagotto and T.M. Rice, 'Science' 271, 618 (1996).  
 [3] F.D.M. Haldane, Phys. Rev. Lett. 50, 1153 (1983).  
 [4] Z. Hiroi and M. Takano, Nature (London) **377**, 411 (1995).  
 [5] M. Azuma, Z. Hiroi, M. Takano, K. Ishida and Y. Kitaoka, Phys. Rev. Letts. **73**, 3463 (1994).  
 [6] P. W. Anderson, Science **235**, 1196 (1987).  
 [7] F.C. Zhang and T.M. Rice, Phys. Rev. **B37**, 3759 (1988).  
 [8] E. Dagotto, J. Riera and D.J. Scalapino, Phys. Rev. **45**, 5744 (1992).  
 [9] H. Tsunetsugu, M. Troyer and T.M. Rice, Phys. Rev. **B49**, 16078 (1994).  
 [10] M. Troyer, H. Tsunetsugu and T.M. Rice, Phys. Rev. **B53**, 251 (1996).  
 [11] D. Poilblanc, D.J. Scalapino and W. Hanke, Phys. Rev. **B52**, 6796 (1995).  
 [12] C.A. Hayward and D. Poilblanc, Phys. Rev. **B53**, 11721 (1996).  
 [13] C.A. Hayward, D. Poilblanc and D.J. Scalapino, Phys. Rev. **B53**, R8863 (1996).  
 [14] T.F.A. Müller and T.M. Rice, Phys. Rev. **B58**, 3425 (1998).  
 [15] J. Riera, D. Poilblanc and E. Dagotto, Eur. Phys. J. **B7**, 53 (1999).  
 [16] M. Brunner, S. Capponi, F.F. Assaad and A. Muramatsu, Phys. Rev. **B63**, 180511 (2001).  
 [17] S.R. White and D.J. Scalapino, Phys. Rev. **B55**, 6504 (1997).  
 [18] G. Sierra, M.A. Martin-Delgado, J. Dukelsky, S.R. White and D.J. Scalapino, Phys. Rev. **B57**, 11666 (1998).  
 [19] S.R. White and D.J. Scalapino, Phys. Rev. **B57**, 11666 (1998).  
 [20] S. Rommer, S.R. White and D.J. Scalapino, Phys. Rev. **B61**, 13424 (2000).  
 [21] T. Siller, M. Troyer, T.M. Rice and S.R. White, Phys. Rev. **B63**, 195106 (2001).  
 [22] S.R. White, I. Affleck and D.J. Scalapino, Phys. Rev. **B65**, 165122 (2002).  
 [23] U. Schollwock, S. Chakravarty, J.O. Fjaerstad, J.B. Marston and M. Troyer, Phys. Rev. Letts. **90**, 186401 (2003).  
 [24] D. Poilblanc, E. Orignac, S.R. White and S. Capponi, Phys. Rev. **B69**, 220406(R) (2004).  
 [25] O.P. Sushkov, Phys. Rev. **B60**, 3289 (1999).  
 [26] M. Sigrist, T.M. Rice and F.C. Zhang, Phys. Rev. **B49**, 12058 (1994).  
 [27] Y.L. Lee, Y.W. Lee, C.Y. Mou and Z.Y. Weng, Phys. Rev. **B60**, 13418 (1999).  
 [28] W-H. Zheng and C.J. Hamer, Phys. Rev. **B66**, 085112 (2002).  
 [29] J. Oitmaa, C.J. Hamer and Zheng W-H., Phys. Rev. **B60**, 16364 (1999).  
 [30] C. Jurecka and W. Brenig, Physica B - Cond. Mat. **312**, 592 (2002).  
 [31] C.D. Batista and G. Ortiz, Phys. Rev. Letts. **85**, 4755 (2000).  
 [32] T. Barnes, E. Dagotto, A. Moreo and E.S. Swanson, Phys. Rev. **B40**, 10977 (1989).  
 [33] J. Riera and E. Dagotto, Phys. Rev. **B47**, 15346 (1993).  
 [34] A.L. Chernyshev and P.W. Leung, Phys. Rev. **B60**, 1592 (1999).  
 [35] J.A. Riera, Phys. Rev. **B64**, 104520 (2001).  
 [36] Y. Nagaoka, Phys. Rev. **147**, 392 (1966).  
 [37] W.F. Brinkman and T.M. Rice, Phys. Rev. **B2**, 1324 (1970).  
 [38] B.I. Shraiman and E.D. Siggia, Phys. Rev. Letts. **60**, 740 (1988).  
 [39] C.L. Kane, P.A. Lee and N. Read, Phys. Rev. **B39**, 6880 (1989).  
 [40] S.R. White and I. Affleck, Phys. Rev. **B64**, 02411 (2001).  
 [41] H. J. Schulz, Phys. Rev. **B59**, 2471 (1999).  
 [42] S. R. White, Phys. Rev. Lett. **69**, 2863 (1992); Phys. Rev. **B48**, 10345 (1993); I. Peschel, X. Wang, M. Kaulke and K. Hallberg (eds), *Density Matrix Renormalization*, Springer (1999).  
 [43] G. Martinez and P. Horsch, Phys. Rev. **B44**, 317 (1991).  
 [44] Z. Liu and E. Manousakis, Phys. Rev. **B45**, 2425 (1992).  
 [45] C.J. Hamer, Zheng W-H. and J. Oitmaa, Phys. Rev. **58**, 15508 (1998).  
 [46] S. Schmitt-Rink, C.M. Varma and A.E. Ruckenstein, Phys. Rev. Lett. **60**, 2793 (1988).  
 [47] M. Ogata, M. U. Luchini, S. Sorella, F.F. Assaad, Phys. Rev. Lett. **66**, 2388 (1991).